Colloid & Polymer Science Colloid Polym Sci 272:1056–1067 (1994)

General analysis of the measurements of the lateral crystal lattice moduli of semicrystalline polymers by x-ray diffraction and the application to nylon 6

M. Matsuo[1]), Y. Shimizu[1]), Y. Harashina[1]), and T. Ogita[2])

[1]) Department of Textile and Apparel Science, Faculty of Human Life and Environment, Nara Women's University, Nara, Japan
[2]) Department of Material Engineering, Faculty of Engineering, Yamagata University, Yonezawa, Japan

Abstract: A mathematical representation based on a linear elastic theory is proposed by which one may investigate the dependences of molecular orientation and crystallinity on the crystal lattice moduli and linear thermal expansion coefficients in the direction perpendicular to the chain axis as commonly measured by x-ray diffraction. In the theoretical calculation, a previously introduced model was employed in which oriented crystalline phase is surrounded by oriented amorphous phase and the strains of the two phases at the boundary are identical. The mathematical analysis indicated that the lateral crystal lattice moduli and linear thermal coefficients as measured by x-ray diffraction may be different from the intrinsic crystal moduli and linear thermal coefficients of a crystal unit cell, depending on the structure of the polymer solid. The numerical calculation was applied to nylon 6. As a result, it may be confirmed that the lateral crystal lattice moduli measured by x-ray diffraction are sensitive to the morphology of the bulk specimens and close to the intrinsic crystal moduli if the morphology of the test specimen can be represented by a parallel model with respect to the original stretching longitudinal direction.

Key words: Linear elastic theory – crystal lattice modulus – x-ray diffraction – lateral crystal lattice moduli – nylon 6

I Introduction

It is well known that in crystalline polymers the ultimate values of bulk Young's moduli in the chain axis direction are equivalent to the corresponding values of their crystal lattices. The lattice elastic moduli of a number of oriented crystalline polymers have been determined from the lattice strains obtained from x-ray diffraction measurements [1–12]. An essential question in the determination of the crystal lattice modulus by x-ray measurements is whether or not the critical assumption in this method is valid, i.e., the specimen is under homogeneous stress. To check this concept, mathematical representations based on a linear elastic theory have been proposed by using three-dimensional composite models of crystalline and amorphous phases [13–16] given as a generalization of the classical Takayanagi model [17].

One such model has been applied to a polymeric system that has a low degree of molecular orientation and crystallinity [16]. In that study, it was found that, depending upon the structure of the polymer, the elastic moduli of the crystal lattice as determined by the x-ray diffraction may differ from the corresponding intrinsic values calculated from the positions of molecules within the crystal lattice.

Numerical calculations have been carried out for cellulose [12] and nylon 6 (α-type) [18] using both the intrinsic elastic compliances S_{ij}^{c0} of a crystal unit calculated by Tashiro et al. [19–20] and the crystal orientation factors obtained by Roe and Krigbaum's method [21–23]. It has been found from these calculations that the crystal

lattice moduli determined by the x-ray diffraction closely approach the intrinsic crystal moduli if the morphology of the specimen can be represented by a series model rather than by a parallel model.

While most of the investigations have been concerned with the lattice moduli in the longitudinal direction along the crystal chain axis, relatively little has been done on the lattice moduli in the lateral direction. It may be noted that, unlike the longitudinal moduli in which the intramolecular forces are of primary importance, these lateral moduli are closely related with varying degrees to several kinds of intermolecular force within the crystallite, including hydrogen bonds and van der Waals forces, and to packing models of molecular chains inside the crystal unit. An investigation of the lateral moduli should, therefore, provide some insight about the influence of these factors on the elastic property of polymer crystals. To our knowledge, only a few publications exist that deal with the x-ray measurements of the lateral lattice moduli [24–26]. In those investigations, however, there was some uncertainty about the values because of the use of crude experimental methods and calculations.

The present paper further investigates the crystal lattice moduli in the direction perpendicular to the chain axis. This problem was already investigated by Sakurada et al. using x-ray diffraction [24]. In this system, however, an essential question arises as to whether the crystal lattice moduli as measured by x-ray diffraction are close to their intrinsic values. In order to study this question, the crystal lattice moduli and the linear thermal expansion coefficients perpendicular to the chain axis, as measured by x-ray diffraction, are formulated as a function of crystallinity and molecular orientation. Efforts have been made here to preserve the notation in the previous paper [18].

The numerical calculation is carried out for drawn nylon 6 films so as to check whether the values of the orientation factors and crystallinity may cause significant effects on the values of the crystal lattice modulus derived from x-ray measurements, in addition to a composite mode of crystal and amorphous phases.

Additionally, the stresses used in the measurements of lattice strains of nylon 6 were chosen so as to avoid the preferential orientation of the above-mentioned hydrogen bonded sheets during the tests. The data were then analyzed by means of a method adopted earlier [18] which allowed us to probe not only the influence of morphology, but also of the crystal orientation, as well as of the molecular orientation in the amorphous phase.

II. Theory

A mathematical representation is proposed to estimate the crystal lattice modulus and the linear thermal expansion coefficients perpendicular to the chain axis as well as the Young's modulus and the thermal expansion coefficient of bulk specimen in the transverse direction, as a function of crystallinity and molecular orientation, when the external stress is applied to the test specimen in the transverse direction. The procedure for calculating the mechanical anisotropy of a single-phase system for the orientation of the structural unit is discussed in relation to mutual conversion of the orientation distribution function of the structural unit with respect to Cartesian coordinates fixed within the bulk specimen [18].

Figure 1 shows the composite structural unit, in which oriented crystallites are surrounded by oriented amorphous phase, and amorphous layers are adjacent to oriented crystalline layers with the interfaces perpendicular to the X_1, X_2, and X_3

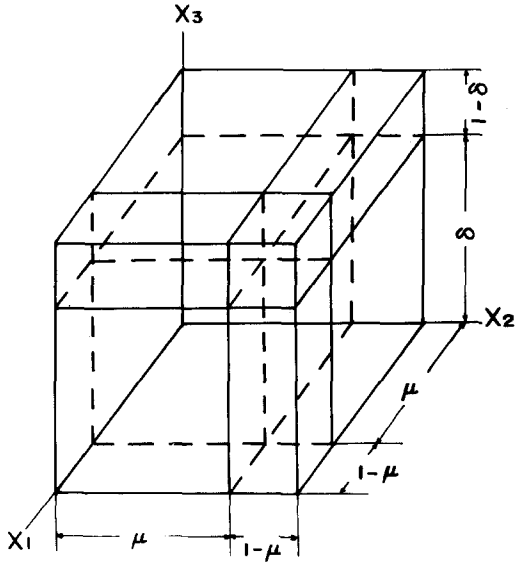

Fig. 1. Composite structural unit of a semicrystalline polymer whose crystallites are surrounded by amorphous phase

axes. The X_3 axis takes along the stretching direction, the X_2 axis along the transverse direction, and the X_1 axis along the film thickness direction. It is assumed that the strains of the two phases at the boundary are identical. This model is thought to be a realistic representation of the morphology of crystalline polymers with a low degree of molecular orientation and a low crystallinity, as pointed by Hibi et al. [27]. The volume crystallinity X_c is represented by $\delta\mu^2$ by use of the fraction lengths δ and μ in the directions of U_3 and U_2 (and U_1) axes, respectively. Incidentally, any other structure such as paracrystalline region is not taken into consideration in this model system.

Using a procedure similar to that discussed in the previous paper [18], this model is constructed by three components as shown in Fig. 2. This analysis is done to formulate generalized Hook's law when the external stress is applied to the transverse direction (the X_2 axis) in this model. In model (a), an anisotropic amorphous layer lies adjacent to the crystallite with the interface perpendicular to the X_2 axis, and in model (b) an anisotropic amorphous layer with fraction length $1-\mu$ is attached to the structure of phase I in a plane normal to the X_1 axis. The final phase III can be constructed by adding an anisotropic layer with fraction length $1-\delta$ to phase II. The procedure is convenient for analysis of the stress-strain relationships in each phase, and the mechanical constants of two phases can be written by using the average mechanical constants of their phases. At $\mu = 1$, this model corresponds to a series model, while at $\delta = 1$, it corresponds to a parallel model. Of course, it is obvious that a series coupling in longitudinal direction requires a parallel coupling in transverse direction. The inverse relationship is also constructed.

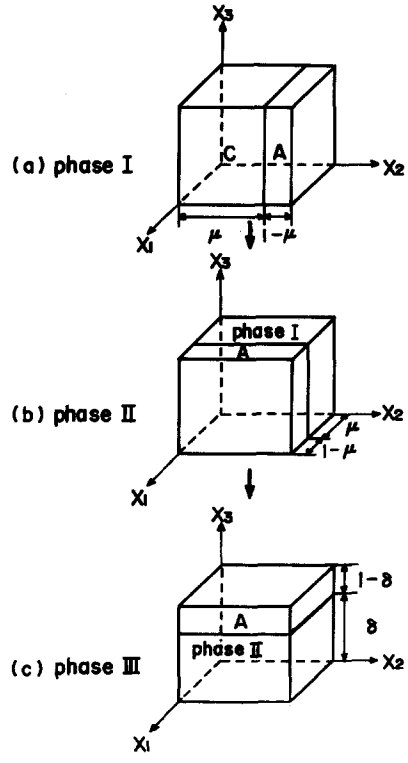

Fig. 2. A procedure to construct a model in Fig. 1; model (a), amorphous phase attached to the X_2 face of the crystallite to construct phase I; model (b), amorphous phase attached to the X_1 face of phase I to construct phase II; model (c), amorphous phase attached to the X_3 face of phase II to construct to the phase III

When the uniaxial external tensile stress σ_{22} is applied along the X_2 axis in model (a) in Fig. 2, the inner stresses of the crystalline and amorphous phases, $(\sigma^c_{11}, \sigma^c_{22}, \sigma^c_{33}, 0, 0, 0)$ and $(\sigma^a_{11}, \sigma^a_{22}, \sigma^a_{33}, 0, 0, 0)$ are applied to the two phases, respectively, including the following strains in the respective phases;

$$\varepsilon^c_{11} = S^{cv}_{11}\sigma^c_{11} + S^{cv}_{12}\sigma^c_{22} + S^{cv}_{13}\sigma^c_{33} + \alpha^{cv}_{11}\Delta T$$
$$\varepsilon^c_{22} = S^{cv}_{12}\sigma^c_{11} + S^{cv}_{11}\sigma^c_{22} + S^{cv}_{13}\sigma^c_{33} + \alpha^{cv}_{11}\Delta T$$
$$\varepsilon^c_{33} = S^{cv}_{13}\sigma^c_{11} + S^{cv}_{13}\sigma^c_{22} + S^{cv}_{33}\sigma^c_{33} + \alpha^{cv}_{33}\Delta T$$
$$\varepsilon^c_{12} = \varepsilon^c_{23} = \varepsilon^c_{31} = 0 \qquad (1)$$

and

$$\varepsilon^a_{11} = S^{av}_{11}\sigma^a_{11} + S^{av}_{12}\sigma^a_{22} + S^{av}_{13}\sigma^a_{33} + \alpha^{av}_{11}\Delta T$$
$$\varepsilon^a_{22} = S^{av}_{12}\sigma^a_{11} + S^{av}_{11}\sigma^a_{22} + S^{av}_{13}\sigma^a_{33} + \alpha^{av}_{11}\Delta T$$
$$\varepsilon^a_{33} = S^{av}_{13}\sigma^a_{11} + S^{av}_{13}\sigma^a_{22} + S^{av}_{33}\sigma^a_{33} + \alpha^{av}_{33}\Delta T$$
$$\varepsilon^a_{12} = \varepsilon^a_{23} = \varepsilon^a_{31} = 0 \qquad (2)$$

Here, S^{cv}_{ij} and S^{av}_{ij} are the average elastic compliances of the crystalline and amorphous phases, respectively, represented by their intrinsic compliances S^{c0}_{ij} and S^{a0}_{ij} and the second and fourth order orientation factors of crystallites and amorphous chain segments, which is described in Eqs. (5) and (6) of ref. [16]. Parameters α^{cv}_{ii} and α^{av}_{ii} represent the average thermal expansion coefficients of the crystalline and amorphous phases, respectively. They can be combined with the intrinsic linear thermal expansion coefficients α^{c0}_{ii} and α^{a0}_{ii}, of the crystal and amorphous phases

by Eqs. (11)–(14) in ref. [16]. ΔT is given by $T - T_0$, where T_0 is the reference temperature. The uniaxial stress condition with respect to the X_2 axis leads to the relations.

$$\sigma_{11}^{I} = \mu\sigma_{11}^{c} + (1-\mu)\sigma_{11}^{a} = 0$$
$$\sigma_{22}^{I} = \sigma_{22}^{c} = \sigma_{22}^{a}$$
$$\sigma_{33}^{I} = \mu\sigma_{33}^{c} + (1-\mu)\sigma_{33}^{a} = 0\,, \tag{3}$$

where σ_{ii}^{I} corresponds to the stress of the bulk specimen.

Because of the above restriction upon the strains, it follows that

$$\varepsilon_{11}^{I} = \varepsilon_{11}^{c} = \varepsilon_{11}^{a}$$
$$\varepsilon_{22}^{I} = \mu\varepsilon_{22}^{c} + (1-\mu)\varepsilon_{22}^{a}$$
$$\varepsilon_{33}^{I} = \varepsilon_{33}^{c} = \varepsilon_{33}^{a}\,. \tag{4}$$

When stresses $(0, \sigma_{22}^{I}, \sigma_{33}^{I}, 0, 0, 0)$ and $(0, \sigma_{22}^{a}, \sigma_{33}^{a}, 0, 0, 0)$ are applied to each layer in model (b), the following strains are induced in the respective phases;

$$\varepsilon_{11}^{I} = S_{12}^{I}\sigma_{22}^{I} + S_{13}^{I}\sigma_{33}^{I} + \alpha_{11}^{I}\Delta T$$
$$\varepsilon_{22}^{I} = S_{22}^{I}\sigma_{22}^{I} + S_{23}^{I}\sigma_{33}^{I} + \alpha_{22}^{I}\Delta T$$
$$\varepsilon_{33}^{I} = S_{23}^{I}\sigma_{22}^{I} + S_{33}^{I}\sigma_{33}^{I} + \alpha_{33}^{I}\Delta T\,, \tag{5}$$

and

$$\varepsilon_{11}^{a} = S_{12}^{av}\sigma_{22}^{a} + S_{13}^{av}\sigma_{33}^{a} + \alpha_{11}^{av}\Delta T$$
$$\varepsilon_{22}^{a} = S_{11}^{av}\sigma_{22}^{a} + S_{13}^{av}\sigma_{33}^{a} + \alpha_{11}^{av}\Delta T$$
$$\varepsilon_{33}^{a} = S_{13}^{av}\sigma_{22}^{a} + S_{33}^{av}\sigma_{33}^{a} + \alpha_{33}^{av}\Delta T\,. \tag{6}$$

Here, one considers a case where the composite unit is subjected to a tensile stress in the direction of the X_2 axis as shown in Fig. 2(b), leaving the other directions free from external force. Under this condition, one obtains

$$\sigma_{11}^{II} = 0$$
$$\sigma_{22}^{II} = \mu\sigma_{22}^{I} + (1-\mu)\sigma_{22}^{a}$$
$$\sigma_{33}^{II} = \mu\sigma_{33}^{I} + (1-\mu)\sigma_{33}^{a} = 0\,. \tag{7}$$

For the above restriction upon the stress, one derives

$$\varepsilon_{11}^{II} = \mu\varepsilon_{11}^{I} + (1-\mu)\varepsilon_{11}^{a}$$
$$\varepsilon_{22}^{II} = \varepsilon_{22}^{I} = \varepsilon_{22}^{a}$$
$$\varepsilon_{33}^{II} = \varepsilon_{33}^{I} = \varepsilon_{33}^{a}\,. \tag{8}$$

The elastic compliances S_{ij}^{I} of the phase I in Eq. (5) can be formulated as a function of S_{ij}^{cv}, S_{ij}^{av} and μ according to the method of Hibi et al. [13], and the thermal expansion coefficients α_{ii}^{I} are written in the Appendix.

When stresses $(\sigma_{11}^{II}, \sigma_{22}^{II}, 0, 0, 0, 0)$ and $(\sigma_{11}^{a}, \sigma_{22}^{a}, 0, 0, 0, 0)$ are applied to each layer in model (c), the following relationships are obtained;

$$\varepsilon_{11}^{II} = S_{11}^{II}\sigma_{11}^{II} + S_{12}^{II}\sigma_{22}^{II} + \alpha_{11}^{II}\Delta T$$
$$\varepsilon_{22}^{II} = S_{12}^{II}\sigma_{11}^{II} + S_{22}^{II}\sigma_{22}^{II} + \alpha_{22}^{II}\Delta T$$
$$\varepsilon_{33}^{II} = S_{13}^{II}\sigma_{11}^{II} + S_{23}^{II}\sigma_{22}^{II} + \alpha_{33}^{II}\Delta T \tag{9}$$

and

$$\varepsilon_{11}^{a} = S_{11}^{av}\sigma_{11}^{a} + S_{12}^{av}\sigma_{22}^{a} + \alpha_{11}^{av}\Delta T$$
$$\varepsilon_{22}^{a} = S_{12}^{av}\sigma_{11}^{a} + S_{11}^{av}\sigma_{22}^{a} + \alpha_{11}^{av}\Delta T$$
$$\varepsilon_{33}^{a} = S_{13}^{av}\sigma_{11}^{a} + S_{13}^{av}\sigma_{22}^{a} + \alpha_{33}^{av}\Delta T\,. \tag{10}$$

The elastic compliances S_{ij}^{II} of phase II can be formulated as a function of S_{ij}^{I}, S_{ij}^{av}, and δ, according to the method of Hibi et al. [27], and the thermal expansion coefficients α_{ii}^{II} are also described in the Appendix. The uniaxial stress condition with respect to the X_2 axis leads to the relations.

$$\sigma_{11}^{III} = \delta\sigma_{11}^{II} + (1-\delta)\sigma_{11}^{a} = 0$$
$$\sigma_{22}^{III} = \delta\sigma_{22}^{II} + (1-\delta)\sigma_{22}^{a} = \sigma_{22}$$
$$\sigma_{33}^{III} = 0\,. \tag{11}$$

For the above restriction upon the strains, one has

$$\varepsilon_{11}^{III} = \varepsilon_{11}^{II} = \varepsilon_{11}^{a}$$
$$\varepsilon_{22}^{III} = \varepsilon_{22}^{II} = \varepsilon_{22}^{a} = \varepsilon_{22}$$
$$\varepsilon_{33}^{III} = \delta\varepsilon_{33}^{II} + (1-\delta)\varepsilon_{33}^{a}\,, \tag{12}$$

where ε_{ii}^{III} and σ_{ii}^{III} correspond to the strain of the bulk specimen and the applied external stress, respectively.

Therefore, we replace ε_{22}^{III} and σ_{22}^{III} as ε_{22} and σ_{22}, respectively.

By use of Eqs. (1)–(12), the bulk strain ε_{22} can be separated into two components; one is $\varepsilon_{22}^{\sigma}$, associated with the external applied stress, and the other is ε_{22}^{T}, associated with the thermal expansion effect. That is,

$$\varepsilon_{22} = \varepsilon_{22}^{\sigma} + \varepsilon_{22}^{T}\,, \tag{13}$$

where

$$\varepsilon_{22}^{\sigma} = \frac{S_{12}^{II} S_{11}^{av} + FC1[S_{22}^{II}\{(1-\delta)S_{12}^{II} + \delta S_{12}^{av}\} - S_{12}^{II}\{(1-\delta)S_{22}^{II} + \delta S_{11}^{av}\}]}{(1-\delta)S_{12}^{II} + \delta S_{12}^{av}} \sigma_{22} \quad (13\text{-a})$$

and

$$\varepsilon_{22}^{T} = \langle\langle (1-\delta)S_{12}^{II}\alpha_{11}^{av} + \delta S_{12}^{av}\alpha_{22}^{II} - FC2[S_{22}^{II}\{(1-\delta)S_{12}^{II} + \delta S_{12}^{av}\} - S_{12}^{II}\{(1-\delta)S_{22}^{II} + \delta S_{11}^{av}\}]\rangle\rangle \Delta T / \{(1-\delta)S_{12}^{II} + \delta S_{12}^{av}\}, \quad (13\text{-b})$$

where the coefficients $FC1$ and $FC2$ are represented in the Appendix. Thus, Young's modulus E in the transverse direction is given by

$$E = \frac{\sigma_{22}}{\varepsilon_{22}^{\sigma}} = \frac{(1-\delta)S_{12}^{II} + \delta S_{12}^{av}}{S_{12}^{II} S_{11}^{av} + FC1[S_{22}^{II}\{(1-\delta)S_{12}^{II} + \delta S_{12}^{av}\} - S_{12}^{II}\{(1-\delta)S_{22}^{II} + \delta S_{11}^{av}\}]} \quad (14)$$

and the thermal expansion coefficient in the bulk, α_{22}, corresponds to $\varepsilon_{22}^{T}/\Delta T$.

The lateral crystal strain can be only detected by x-ray diffraction when the reciprocal lattice vector is parallel to the X_2 axis. Figure 3 shows the result when the b-axis corresponds to the crystal fiber axis in such cases as nylon 6 (α-type), cellulose, and poly(vinyl alcohol). The upper and lower diagrams correspond to the geometries to measure the crystal lattice strains of the (00l) and (h00) planes: In this system, Φ_j specifies the azimuthal angle between the U_2 and X_2 axis, in which the U_2 axis lies along the direction of the reciprocal lattice vector of the (00l) plane. Considering this geometrical arrangement, the lateral crystal lattice strain may be given by using the formula of transformation of strain component.

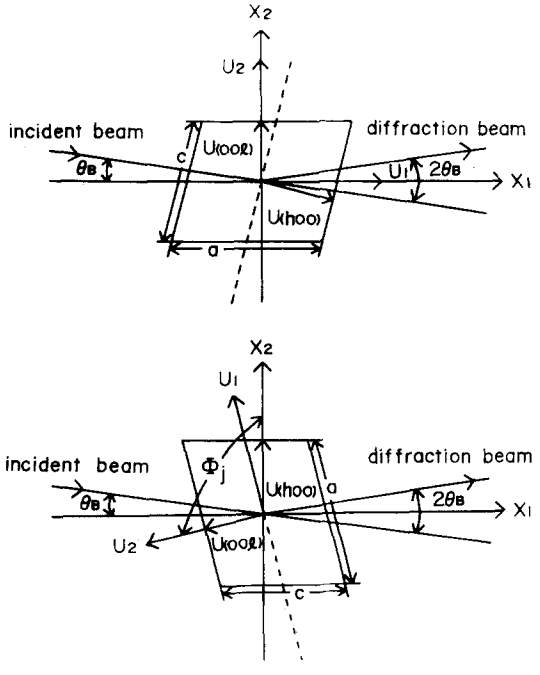

Fig. 3. Geometrical arrangement to detect crystal plane perpendicular to the X_2 axis by x-ray diffraction; (upper diagram) the (00l) plane; (lower diagram) the (h00) plane

$$\varepsilon_{22}^{c}(\Phi_j) = S_{12}^{c0}(\Phi_j)\sigma_{11}^{c} + S_{22}^{c0}(\Phi_j)\sigma_{22}^{c} + S_{23}^{c0}(\Phi_j)\sigma_{33}^{c} + \alpha_{22}^{c0}(\Phi_j)\Delta T, \quad (15)$$

where

$$S_{12}^{c0}(\Phi_j) = \sin^2\Phi_j\cos^2\Phi_j(S_{11}^{c0} + S_{22}^{c0} - S_{66}^{c0}) + (\sin^4\Phi_j + \cos^4\Phi_j)S_{12}^{c0} + \sin\Phi_j\cos\Phi_j(\sin^2\Phi_j - \cos^2\Phi_j)(S_{16}^{c0} - S_{26}^{c0}) \quad (15\text{-a})$$

$$S_{22}^{c0}(\Phi_j) = \sin^4\Phi_j S_{11}^{c0} + \cos^4\Phi_j S_{22}^{c0} + \sin^2\Phi_j\cos^2\Phi_j(2S_{12}^{c0} + S_{66}^{c0}) - 2\sin\Phi_j\cos\Phi_j(\sin^2\Phi_j S_{16}^{c0} + \cos^2\Phi_j S_{26}^{c0}) \quad (15\text{-b})$$

$$S_{23}^{c0}(\Phi_j) = \sin^2\Phi_j S_{13}^{c0} + \cos^2\Phi_j S_{23}^{c0} - \sin\Phi_j\cos\Phi_j S_{36}^{c0} \quad (15\text{-c})$$

and

$$\alpha_{22}^{c}(\Phi_j) = \sin^2\Phi_j\alpha_{11}^{c0} + \cos^2\Phi_j\alpha_{22}^{c0} - 2\sin\Phi_j\cos\Phi_j\alpha_{12}^{c0}. \quad (15\text{-d})$$

As an example, Φ_j for nylon 6 (α-type), becomes 0° and 112.5° for the (002) and (200) planes, respectively.

Here, we can replace σ_{ij}^{c0} as a function of σ_{22}. Thus, Eq. (15) can be rewritten as follows;

$$\varepsilon_{22}^{c}(\Phi_j) = S_{rj}^{c}\sigma_{22} + \alpha_{rj}^{c}\Delta T = \varepsilon_{rj}^{c}(\sigma) + \varepsilon_{rj}^{c}(\Delta T)\,, \tag{16}$$

where

$$S_{rj}^{c} = U_1 S_{12}^{c0}(\Phi_j) + U_2 S_{22}^{c0}(\Phi_j) + U_3 S_{23}^{c0}(\Phi_j) \tag{17}$$

and

$$\alpha_{rj}^{c} = V_1 S_{12}^{c0}(\Phi_j) + V_2 S_{22}^{c0}(\Phi_j) + V_3 S_{23}^{c0}(\Phi_j)\,. \tag{18}$$

All coefficients in Eqs. (17) and (18) are given in the Appendix.

The thermal expansion coefficient of the j-th crystal plane as measured by x-ray diffraction is defined as α_{rj}^{c} and the crystal lattice modulus of the j-th plane may be defined as

$$E_j^{c} = 1/S_{rj}^{c}\,. \tag{19}$$

Here, we must emphasize that E_{rj}^{c} and α_{rj}^{c}, as detected by x-ray diffraction, are different from their intrinsic values $1/S_{22}^{c0}$ and α_{22}^{c0} in a crystal unit.

As shown in Fig. 3, the values of E_{rj}^{c} and α_{rj}^{c} can be estimated experimentally from the measurement of the x-ray intensity distribution by using an ordinary horizontal scanning type goniometor over a desirable range of twice the Bragg angle $2\theta_B$, in which the scanning speed of specimen is half of that of diffractometer. For abbreviation, E_{rj}^{c} is described as E^c in the following chapter.

III. Application to nylon 6

Experimental section

Specimens were prepared from nylon 6 pellets having an average molecular weight of 8.4×10^4. Compression molded films, each about 250 μm in thickness, were obtained by heating the pellets in a hot press at 245 °C for 15 min followed by quenching in ice water to minimize the crystallinity in the films. The films were uniaxially drawn at 190 °C and in the nitrogen environment to a draw ratio λ, of 4. This particular draw ratio was chosen because films having higher draw ratios tended to split along the stretching direction during the lattice strain measurement (even at stress less than 3 MPa) while those having lower draw ratios did not generate sufficient levels of x-ray signals from the crystal (200) and (002) planes.

The films were then heat-set at 200 °C for 20 min and slowly cooled down to room temperature while being maintained at fixed lengths. Strips with a length of about 34 mm were cut across the initial draw axis and subjected to the lattice strain measurements at a gauge length of 7 mm.

Lattice strains in the [200] and [002] directions were measured by x-ray diffraction using Cukα radiation from a rotating anode x-ray tube (Rigaku RDA-rA) operating at 200 mA and 40 kV. The incident beam was collimated to 2 mm in diameter and monochromatized using a curved graphite monochromator. The diffraction beam was passed through a square slit of 0.9 mm × 0.9 mm before reaching the counter. The intensity peaks from the crystal planes were measured at 0.05° intervals over a time period of 10 s in the 2θ range of 19.0 to 21.4° for the (200) planes and 22.3 to 25.2° for the (002) planes. The change of the peak position with respect to the applied stress was measured from the shift in the position of center of mass of the intensity peak [8].

To ensure sufficient levels of diffraction intensity for accurate measurements of lattice strains, it was necessary to have random orientation of both the (200) and (002) planes about the initial draw axis. It was found, however, that some specimens tended to have preferential orientation of these planes parallel to the film surface after the stretching and heat-set treatment. Therefore, only those specimens which showed nearly complete ring patterns in the edge view were used in this experiment.

Another point to be noted here is the peak intensity for the (002) planes which decreased considerably when the applied stress exceeded 13 MPa, apparently because larger stresses tended to cause preferential alignment of the (002) planes parallel to the film surface. Since the decrease was large enough to affect the accuracy of the peak position determination, the applied stress was limited to less than 13 MPa for measurement of the (002) peak positions. The peak intensity for the (200) planes was not

sensitive to the applied stress until the stress exceeded the yield point of about 25 MPa; therefore, measurements for the (200) peak were carried out up to the yield limit.

Orientation of the reciprocal lattice vector of the j-th crystal plane was determined from the corresponding intensity peak. Orientation of the amorphous chain segments was obtained from the birefringence by subtracting the contribution of the crystalline fraction from the total birefringence of the bulk specimen (ca. 6×10^{-3}). Details of this calculation have been described in ref. [18].

Volume crystallinities of the films were found to be in the range of 42 to 46%. These values were calculated from densities measured with a pycnometer, and from the densities data of crystalline (1.23) [28] and amorphous (1.09) [29] fractions.

Results and discussion

Data obtained from the strain measurements are recorded together with the corresponding stress applied to the bulk specimen. The stresses acting on the crystal surfaces are assumed to be the same as the stress being applied to the bulk specimen under the homogeneous stress hypothesis. Typical results obtained from one film specimen are shown in Figs. 4 and 5 where the applied stresses are plotted as functions of measured strains in the [200] and [002] directions. A linear relationship is observed in both plots for stresses up to the limits specified in the Experimental section. The deviation from linearity in the [200] plot at larger stresses is clearly attributable to yielding and, therefore, was not included in the determination of lattice modulus.

In Table 1, we summarize the lattice moduli determined from similar plots for each specimen. Also shown in this table are values of the Young's modulus measured from the bulk specimens in the direction normal to the initial draw axis. It is seen that the lattice modulus is between 11.4 and 12 GPa in the [200] direction and between 7.7

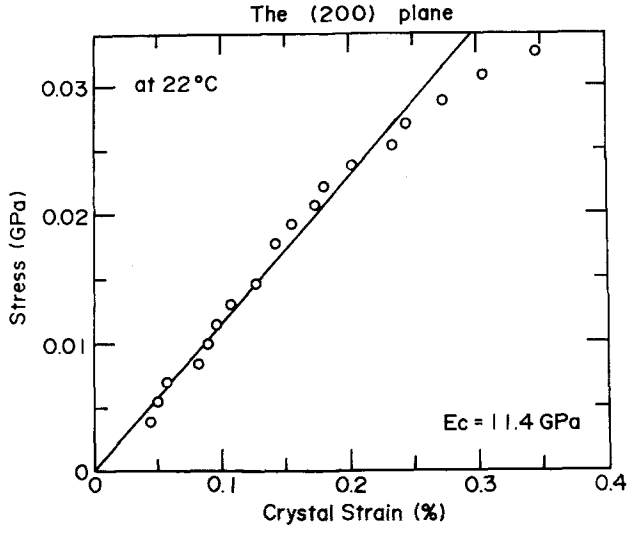

Fig. 4. Relationship between the crystal lattice strain of the (200) plane and the external stress

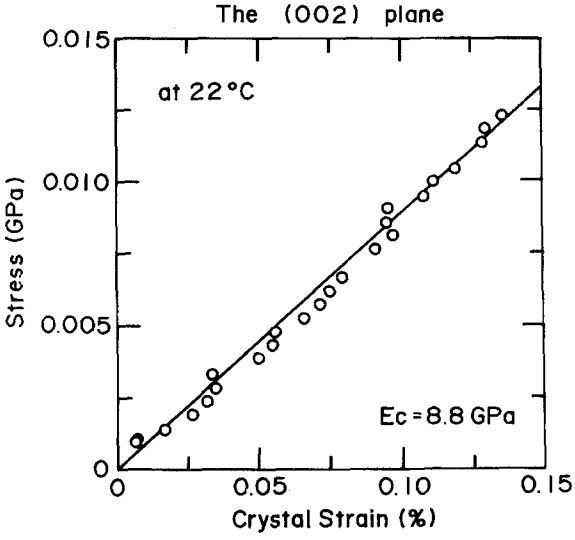

Fig. 5. Relationship between the crystal lattice strain of the (002) plane and the external stress

Table 1. Crystal lattice moduli of the (200) and (002) planes and the Young's modulus of nylon 6

Sample	Crystal lattice modulus (GPa)		Young's modulus (GPa)
	(200)	(002)	
1	11.7	–	1.18
2	11.7	–	1.20
3	11.7	–	1.42
4	11.4	–	1.40
5	12.0	–	1.54
6	–	9.0	1.30
7	–	8.2	1.23
8	–	8.8	1.31
9	–	9.0	1.50
10	–	7.7	1.32

and 9.0 GPa in the [002] direction. The larger values in the [200] direction clearly indicate the strong influence of hydrogen bonds which are aligned in the c-axis direction. A similar observation was made by Tashiro et al. [20] in their theoretical calculation of lattice moduli of nylon 6.

It may be noted that modulus values shown in Table 1 differ substantially from those obtained by Sakurada et al. [24] (7.15 GPa in the [200] direction and 4.31 GPa in the [002] direction.) and by Boukal [25] (6.56 GPa in the [200] direction and 3.23 GPa in the [002] direction.) As briefly noted in the Introduction section, their measurements were handicapped by the use of either unoriented specimens [24] or doubly oriented ones (with the hydrogen bonded sheets oriented parallel to the film surface) which tended to lower the precision of lattice strain measurements in the [002] direction. The deficiency in the latter work [24] was further compounded by the assumptions made in the calculation of the lattice, namely, the crystallinity is 100% and the crystal has a Poisson's ratio of 1/3. For this reason, we believe the values reported by the previous workers are not as reliable as ours.

As discussed in a previous paper [18], the theoretical values of S_{ij}^{c0} that take into account the torsional bonds have not been reported. It is therefore necessary to determine the measurable crystal lattice modulus E_c in the transverse direction by using the values of intrinsic elastic compliances S_{ij}^{c0} calculated by Tashiro et al. [20] for the crystal unit of all-trans planar zig-zag conformation system. However, as the measurable value of E_c by x-ray diffraction depends on the morphology of the specimen, we shall normalize E_c by means of E_c^0 ($= 1/S_{22}^{c0}$) so that we may probe the dependence of E_c on molecular orientation and crystallinity using the composite model of Fig. 1. To this end the crystal orientation factors F_{l0n} ($2 \leqq l \leqq 4$ and $0 \leqq n \leqq 4$) and G_{l0n} ($2 \leqq l \leqq 4$, $n \leqq 4$) of the specimens A ($\lambda = 5$) and B ($\lambda = 4$) were estimated from the x-ray diffraction using the procedure described elsewhere [18]. The orientation factors F_{l00}^{am} ($2 \leqq l \leqq 4$) of the amorphous chain segments and the crystallinity were estimated in accordance with the procedure proposed by Roe and Krigbaum [21–23]. It should be pointed out that the numerical calculation for the specimen A ($\lambda = 5$) was carried out for the purpose of comparison (with specimen B) only since, as noted earlier, there are no data available from this specimen which broke readily and could not be subjected to mechanical tests.

To carry out the above calculation, the elastic compliance S_{11}^{a0} ($= S_{22}^{a0}$) of the amorphous phase was estimated by the double differentation of Lennard–Jones potential energy function while the compliance S_{33}^{a0} was estimated by assuming that the modulus along the chain axis is proportional to the number of molecular chains in the unit area perpendicular to the chain axis [16, 18]. The shear compliances S_{12}^{a0} and S_{13}^{a0} were given by $-\nu_{21}^{a0} S_{11}^{a0}$ ($= \nu_{31}^{a0} S_{11}^{a0}$) and $-\nu_{31}^{a0} S_{33}^{a0}$, respectively. Additionally, the compliance S_{55}^{a0} was estimated from the following expression [18].

$$2S_{11}^{a0} = (2S_{13}^{a0} + S_{55}^{a0})\Omega, \tag{20}$$

where Ω is an adjustable parameter [13] having a range of 0.6 to 1.0 [16, 18].

Our numerical calculations using μ, Ω, and ν_{31}^{a0} as parameters showed that both the lateral Young's modulus and the lateral lattice modulus were not sensitive to changes in ν_{31}^{a0}. Accordingly, the value of ν_{31}^{a0} was fixed at the common value of 0.33.

From Eq. (15-b) and the values of elastic compliances of the unit cells given by Tashiro and Tadokoro [20] for the all-trans planar zig-zag conformation system, we found the lattice modulus to be 16.6 GPa in the [200] direction and 4.61 GPa in the [002] direction. It may be noted that these values differ from the corresponding values listed in Table 1, apparently because the chain structure inside the crystal unit is not truly planar zig-zag as assumed, but it tends to be somewhat contracted at room temperature.

In Fig. 6 we show the lateral bulk Young's modulus, E, calculated from the orientation factors and crystallinity of types A and B specimens as a function of μ. It can be seen that in both types of specimen, E decreases almost linearly with increasing μ while it increases with increasing Ω over the entire range of μ. It is also noted that the value of E is more sensitive to the parameter Ω than to μ in type B ($\lambda = 4$) specimens. On the other hand, E is less sensitive to μ than to Ω in type A ($\lambda = 5$) specimens. The high sensitivity of type A specimens to μ is clearly brought about by the higher degree of molecular orientation in the

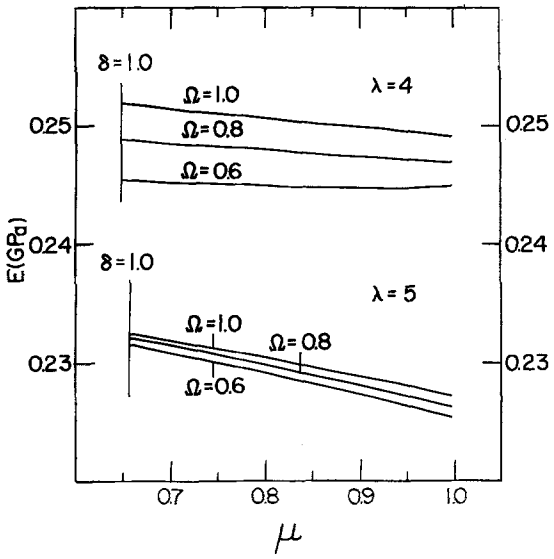

Fig. 6. μ-dependence of Young's modulus E calculated for the specimens A ($\lambda = 5$) and B ($\lambda = 4$)

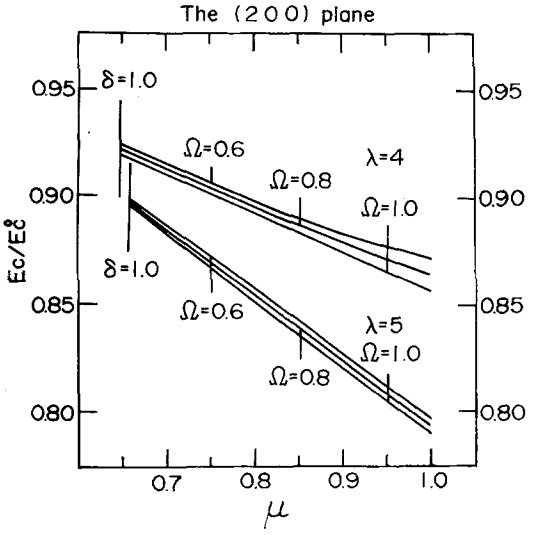

Fig. 7. Ratio E_c/E_c^0 vs. μ calculated for the (200) plane of the specimens A ($\lambda = 5$) and B ($\lambda = 4$)

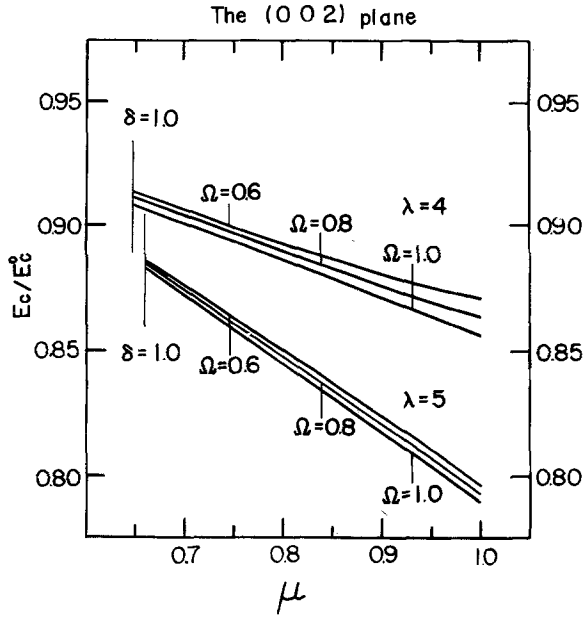

Fig. 8. Ratio E_c/E_c^0 vs. μ calculated for the (002) plane of the specimens A ($\lambda = 5$) and B ($\lambda = 4$)

initial stretching direction (i.e., in the X_3 direction). Therefore, our numerical calculation indicates that E becomes less sensitive to μ as the molecular orientation in the crystalline and amorphous phases turns poorer. This result suggests that two specimens having the same crystallinity and the same molecular orientation may have different lateral bulk Young's moduli depending on how the crystalline and amorphous phases are disposed within the specimens. In other words, unlike the ultra-drawn specimens in which the morphology is relatively simple and can be accounted for easily, the less well oriented specimens such as the ones used in the present experiment have complex morphology and, therefore, it cannot be accounted for as readily in the determination of the bulk moduli.

In Figs. 7 and 8, we show the ratio of E_c/E^0 as function of μ for three different values of Ω in the [200] (Fig. 7) and [002] (Fig. 8) directions. The decreasing trend of E_c/E^0 with increasing μ in both figures indicates that the lateral crystal lattice moduli, as measured by x-ray diffraction, are below the intrinsic values and furthermore, the discrepancy becomes more pronounced as μ increases. It is also noted from comparison with the results in Fig. 4 that of the two quantities, E and the ratio E_c/E^0, the latter is more sensitive to μ.

The results in Figs. 7 and 8 also indicate that for Ω in the range of 0.6 to 1.0, our experimental values contain maximum errors (at $\mu = 1$) between 13 and 15% for type B specimens and between 20 to 22% for type A specimens. Thus, type B specimens are more suitable than type A specimens for determining the lateral crystal lattice moduli. Additionally, as the errors in Figs. 7 and 8 are at their minima when $\delta = 1$, it

may be inferred that the influence of parallel coupling between the amorphous and crystalline phases is stronger when the stress is applied in the X_2 direction. As discussed before, it is evident that a parallel coupling ($\delta = 1$) in longitudinal direction (i.e., the X_3 axis) corresponds to a series coupling in transverse direction (i.e., the X_2 axis).

Before closing, we note that it is, in general, difficult to determine correct values of the lateral lattice moduli of polymeric materials by the x-ray technique because the low fracture strength of the highly oriented specimens in the lateral direction necessitates the use of less well oriented specimens which are less amenable to analysis because of their complex morphological details. Nevertheless, it should be pointed out that our values are closer to the real values than those reported by Sakurada et al. [24], because in their experiment they could not directly measure the lattice strain in the X_2 direction and had to estimate the lattice moduli by resorting to a crude approximation which is not suitable for polymers such as nylon 6 which has low degrees of crystallinity and molecular orientation.

IV. Conclusion

Theoretical calculations in the determination of the crystal lattice moduli by x-ray diffraction were carried out as a function of molecular orientation and crystallinity. In this calculation, a model was employed in which oriented crystalline layers are surrounded by oriented amorphous phase and the strains of the two phases at the boundary are identical. It was found that the crystal lattice modulus E_c measured by x-ray diffraction is dependent upon the morphological properties of the test specimen and is not equal to the intrinsic value E_c^0.

To check the morphological dependence of the lateral lattice moduli, the crystal lattice moduli of uniaxially oriented nylon 6 were measured in the direction normal to the crystal chain axis using x-ray diffraction. The measurements involved determination of lattice strains in the [200] and [002] directions as well as the molecular orientation factors of the crystalline and amorphous regions. Values of the moduli were found to be between 11.4 and 12.0 GPa in the [200] direction and between 7.7 and 9.0 GPa in the [002] direction. The difference in the modulus between the two directions reflects the influence of secondary intermolecular interactions which are dominated by hydrogen bonding forces in the [200] direction and van der Waals. forces in the [002] direction. Our calculations using a three-dimensional two-phase block model showed that, as far as the lateral moduli are concerned, there is a significant degree of parallel coupling between the amorphous and crystalline phases and that, depending on the degree of this mechanical coupling, the moduli could differ by 12 to 15% from the corresponding values calculated by Tashiro et al. [20] based on lattice potential functions. The parallel coupling arose from the use of specimens having a relatively low degree of molecular orientation ($\lambda = 4$) which was necessary in order to avoid splitting of specimens along the draw axis during the modulus measurements.

Appendix

The thermal coefficients α_{ii}^{I} in Eq. (5) and α_{ii}^{II} in Eq. (9) may be given by

$$\alpha_{11}^{I} = \alpha_{11}^{cv} - S_{11}^{cv} FA3 - S_{13}^{cv} FA4 \tag{A-1}$$

$$\alpha_{22}^{I} = \mu\alpha_{11}^{cv} + (1-\mu)\alpha_{11}^{av} - \mu\{(S_{12}^{cv} - S_{12}^{av})FA3 + (S_{13}^{cv} - S_{13}^{av})FA4\} \tag{A-2}$$

$$\alpha_{33}^{I} = \alpha_{33}^{cv} - S_{13}^{cv} FA3 - S_{33}^{cv} FA4 \tag{A-3}$$

$$\begin{aligned}\alpha_{11}^{II} = {} & \mu\alpha_{11}^{I} + (1-\mu)\alpha_{11}^{av} - \mu(S_{12}^{I} - S_{12}^{av})FB2 \\ & + \mu\left(\frac{S_{13}^{I}}{S_{13}^{av}} - 1\right) \\ & \times [(1-\mu)\{\alpha_{11}^{cv} - \alpha_{11}^{av} - (S_{12}^{cv} - S_{12}^{av})FB2\} \\ & - \{(1-\mu)S_{11}^{cv} + \mu S_{11}^{av}\}(FA3 + FB2 \cdot FA1) \\ & - \{(1-\mu)S_{13}^{cv} + \mu S_{13}^{av}\}(FA4 + FB2 \cdot FA2)]\end{aligned} \tag{A-4}$$

$$\begin{aligned}\alpha_{22}^{II} = {} & \mu\alpha_{11}^{cv} + (1-\mu)\alpha_{11}^{av} \\ & - FB2\{\mu S_{11}^{cv} + (1-\mu)S_{11}^{av}\} \\ & - \mu(S_{12}^{cv} - S_{12}^{av})(FA3 + FB2 \cdot FA1) \\ & - \mu(S_{13}^{cv} - S_{13}^{av})(FA4 + FB2 \cdot FA2)\end{aligned} \tag{A-5}$$

$$\begin{aligned}\alpha_{33}^{II} = {} & \alpha_{33}^{cv} - S_{13}^{cv} FA3 - S_{33}^{cv} FA4 \\ & - FB2(S_{13}^{cv} FA1 + S_{13}^{cv} + S_{33}^{cv} FA2)\,,\end{aligned} \tag{A-6}$$

where

$$FA1 = \frac{\left(S_{33}^{cv} + \frac{\mu}{1-\mu} S_{33}^{av}\right)(S_{12}^{cv} - S_{12}^{av}) - \left(S_{13}^{cv} + \frac{\mu}{1-\mu} S_{13}^{av}\right)(S_{13}^{cv} - S_{13}^{av})}{\left(S_{13}^{cv} + \frac{\mu}{1-\mu} S_{13}^{av}\right)^2 - \left(S_{11}^{cv} + \frac{\mu}{1-\mu} S_{11}^{av}\right)\left(S_{33}^{cv} + \frac{\mu}{1-\mu} S_{33}^{av}\right)} \tag{A-7}$$

$$FA2 = \frac{\left(S_{11}^{cv} + \frac{\mu}{1-\mu} S_{11}^{av}\right)(S_{13}^{cv} - S_{13}^{av}) - \left(S_{13}^{cv} + \frac{\mu}{1-\mu} S_{13}^{av}\right)(S_{12}^{cv} - S_{12}^{av})}{\left(S_{13}^{cv} + \frac{\mu}{1-\mu} S_{13}^{av}\right)^2 - \left(S_{11}^{cv} + \frac{\mu}{1-\mu} S_{11}^{av}\right)\left(S_{33}^{cv} + \frac{\mu}{1-\mu} S_{33}^{av}\right)} \tag{A-8}$$

$$FA3 = \frac{\left(S_{13}^{cv} + \frac{\mu}{1-\mu} S_{13}^{av}\right)(\alpha_{33}^{cv} - \alpha_{33}^{av}) - \left(S_{33}^{cv} + \frac{\mu}{1-\mu} S_{33}^{av}\right)(\alpha_{11}^{cv} - \alpha_{11}^{av})}{\left(S_{13}^{cv} + \frac{\mu}{1-\mu} S_{13}^{av}\right)^2 - \left(S_{11}^{cv} + \frac{\mu}{1-\mu} S_{11}^{av}\right)\left(S_{33}^{cv} + \frac{\mu}{1-\mu} S_{33}^{av}\right)} \tag{A-9}$$

$$FA4 = \frac{\left(S_{13}^{cv} + \frac{\mu}{1-\mu} S_{13}^{av}\right)(\alpha_{11}^{cv} - \alpha_{11}^{av}) - \left(S_{11}^{cv} + \frac{\mu}{1-\mu} S_{11}^{av}\right)(\alpha_{33}^{cv} - \alpha_{33}^{av})}{\left(S_{13}^{cv} + \frac{\mu}{1-\mu} S_{13}^{av}\right)^2 - \left(S_{11}^{cv} + \frac{\mu}{1-\mu} S_{11}^{av}\right)\left(S_{33}^{cv} + \frac{\mu}{1-\mu} S_{33}^{av}\right)} \tag{A-10}$$

$$FB1 = \frac{\left(S_{33}^{I} + \frac{\mu}{1-\mu} S_{33}^{av}\right) S_{11}^{av} - \left(S_{23}^{I} + \frac{\mu}{1-\mu} S_{13}^{av}\right) S_{13}^{av}}{(1-\mu)\left[\left(S_{33}^{I} + \frac{\mu}{1-\mu} S_{33}^{av}\right)\left(S_{22}^{I} + \frac{\mu}{1-\mu} S_{11}^{av}\right) - \left(S_{23}^{I} + \frac{\mu}{1-\mu} S_{13}^{av}\right)^2\right]} \tag{A-11}$$

$$FB2 = \frac{\left(S_{33}^{I} + \frac{\mu}{1-\mu} S_{33}^{av}\right)(\alpha_{22}^{I} - \alpha_{11}^{av}) - \left(S_{23}^{I} + \frac{\mu}{1-\mu} S_{13}^{av}\right)(\alpha_{33}^{I} - \alpha_{33}^{av})}{\left(S_{33}^{I} + \frac{\mu}{1-\mu} S_{33}^{av}\right)\left(S_{22}^{I} + \frac{\mu}{1-\mu} S_{11}^{av}\right) - \left(S_{23}^{I} + \frac{\mu}{1-\mu} S_{13}^{av}\right)^2}. \tag{A-12}$$

The coefficients $FC1$ in Eq. (13-a) and $FC2$ in Eq. (13-b) may be given by

$$FC1 = \frac{\left(S_{12}^{II} + \frac{\delta}{1-\delta} S_{12}^{av}\right) S_{12}^{av} - \left(S_{11}^{II} + \frac{\delta}{1-\delta} S_{11}^{av}\right) S_{11}^{av}}{(1-\delta)\left[\left(S_{12}^{II} + \frac{\delta}{1-\delta} S_{12}^{av}\right)^2 - \left(S_{11}^{II} + \frac{\delta}{1-\delta} S_{11}^{av}\right)\left(S_{22}^{II} + \frac{\delta}{1-\delta} S_{11}^{av}\right)\right]} \tag{A-13}$$

and

$$FC2 = \frac{\left(S_{12}^{II} + \frac{\delta}{1-\delta} S_{12}^{av}\right)(\alpha_{11}^{II} - \alpha_{11}^{av}) - \left(S_{11}^{II} + \frac{\delta}{1-\delta} S_{11}^{av}\right)(\alpha_{22}^{II} - \alpha_{11}^{av})}{\left(S_{12}^{II} + \frac{\delta}{1-\delta} S_{12}^{av}\right)^2 - \left(S_{11}^{II} + \frac{\delta}{1-\delta} S_{11}^{av}\right)\left(S_{22}^{II} + \frac{\delta}{1-\delta} S_{11}^{av}\right)}. \tag{A-14}$$

The coefficients U_i ($i = 1 \sim 3$) in Eq. (17) and V_i ($i = 1 \sim 3$) in Eq. (18) may be given by

$$U_1 = FA1 \cdot FB1 \cdot FC1 \quad \text{(A-15)}$$

$$U_2 = FB1 \cdot FC1 \quad \text{(A-16)}$$

$$U_3 = FB1 \cdot FC1 \cdot FA2 \quad \text{(A-17)}$$

$$V_1 = -(FA3 + FA1 \cdot FB2 + FA1 \cdot FB1 \cdot FC2) \quad \text{(A-18)}$$

$$V_2 = -(FB2 + FB1 \cdot FC2) \quad \text{(A-19)}$$

$$V_3 = -(FA4 + FA2 \cdot FB2 + FB1 \cdot FA2 \cdot FC2) \quad \text{(A-20)}$$

References

1. Skurada I, Nukushina Y, Ito T (1962) J Polym Sci 57:651
2. Sakurada I, Ito T, Nakamura K (1966) J Polym Sci, Part C 15:75
3. Clements J, Jakeways R, Ward IM (1978) Polymer 19:639
4. Brew B, Clements J, Davies GR, Jakeways R, Ward IM (1979) J Polym Sci Polym Phys Ed 17:351
5. Miyasaka K, Isomoto T, Koganeya H, Uehara K, Ishikawa K (1980) J Polym Sci Polym Phys Ed 18:1047
6. Nakamae K, Nishino T, Hata K, Matsumoto T (1987) Kobunshi Ronbunshu 44:421
7. Thistlethwaite Y, Jakeways R, Ward IM (1988) Polymer 29:61
8. Matsuo M, Sawatari C (1986) Macromolecules 19:2036
9. Sawatari C, Matsuo M (1986) Macromolecules 19:2653
10. Matsuo M, Sawatari C (1988) Macromolecules 21:1653
11. Sawatari C, Matsuo M (1989) Macromolecules 22:2968
12. Matsuo M, Sawatari C, Iwai Y, Ozaki F (1990) Macromolecules 23:3266
13. Hibi S, Maeda M, Mizuno M, Nomura S, Kawai H (1973) Sen-i Gakkaishi 29:729
14. Sawatari C, Matsuo M (1986) Macromolecules 19:2726
15. Matsuo M, Sawatari C (1988) Macromolecules 21:1658
16. Matsuo M (1990) Macromolecules 23:3261
17. Takayanagi M (1963) Mem Fac Eng Kyushu Univ 23:50
18. Matsuo M, Satoh R, Shimizu Y (1993) Colloid & Polym Sci 271:11
19. Tashiro K, Kobayashi M (1988) Polymer Prepr Jpn 37:3017
20. Tashiro K, Tadokoro H (1981) Macromolecules 14:781
21. Roe RJ, Krigbaum, WR (1964) J Chem Phys 40:2608
22. Krigbaum WR, Roe RJ (1964) J Chem Phys 41:737
23. Roe RJ (1965) J Appl Phys 36:2024
24. Sakurada I, Kaji K, Nakamae K (1969) Kobunshi Kagaku 26:833

The value E_c for the (200) plane was given by Sakurada et al. as follows:

$$E_c = (\cos^2 \phi - \nu \sin^2 \phi) E_c' ,$$

where ϕ is the tilting angle, ν, the Poisson's ratio given by $-(S_{12}^{co}/S_{22}^{co})$, and E_c', the apparent crystal modulus measured by x-ray diffraction technique. The above equation, however, can be constructed only in the case when the chains are fully aligned and the specimen is almost completely crystalline.

25. Boukal IJ (1967) Appl Polym Sci 11:1483
26. Sakurada I, Kaji K (1970) J Polym Sci C31:57
27. Maeda M, Hibi S, Itoh F, Nomura S, Kawaguchi T, Kawai H (1970) J Polym Sci Polym Phys Ed 8:1303
28. Holms DR, Bunn CW, Smith DJ (1955) J Polym Sci 17:159
29. Balcerzyk E, Kozlowski W, Wesolowska E, Lewaszkiewicz W (1981) J Appl Polym Sci 26:2573

Received July 28, 1993;
accepted January 17, 1994

Authors' address:

Prof. Masaru Matsuo
Dept. of Clothing Science
Faculty of Home Economics
Nara Women's University
Nara 630, Japan